Article:
Ingham-Dempster, T.A., Rosser, R., Corfe, B.M. et al. (1 more author) (2020) From cell to multi-crypt: Agent-based models of the human colon suggests novel processes of field cancerisation. Journal of Computational Science. 101066. ISSN 1877-7503

https://doi.org/10.1016/j.jocs.2019.101066

From Cell to Multi-crypt: Agent-based Models of the Human Colon Suggests Novel Processes of Field Cancerisation

Timothy A. Ingham-Dempster[1,2,3], Ria Rosser[2], Bernard M. Corfe,[1,2], and Dawn C. Walker[*,1,3]

[1]*INSIGNEO Institute, University of Sheffield, The Pam Liversidge Building, Mappin Street, Sheffield, S1 3JD, UK*

[2]*Molecular Gastroenterology Research Group, Department of Oncology and Metabolism, The Medical School, University of Sheffield, Beech Hill Road, Sheffield, S10 2RX, UK*

[3]*Department of Computer Science, University of Sheffield, Regent Court, 211 Portobello, Sheffield, S1 4DP, UK*

* Corresponding author

Email d.c.walker@sheffield.ac.uk

Abstract

Colorectal cancer (CRC) is a major cause of cancer mortality. It is known that loss of APC gene function through mutation is followed by the expansion of a field of mutated tissue, but the mechanisms behind this expansion are poorly understood.

This study aimed to examine the processes involved in field expansion using two agent-based computational models: a cell-scale model allowing mapping of Apc-mutated cell expansion in small multcrypt arrays, and a tissue-scale model allowing simulation of the entire colon over oncologically relevant timescales.

The cell scale model predicts that mutated cells spread through the flat mucosa of the simulated tissue without invading neighbouring crypts - a process not previously hypothesised in the literature. The crypt-scale model's predictions of field sizes correspond to those estimated in the literature from *in vivo* studies. Our dual-scale modelling approach renders the spatial and temporal scales at which field cancerisation processes occur *in vivo* accessible to exploration by simulation for the first time.

Highlights

- We present novel multiple-scale agent-based models of the colon, where agents are used to represent both individual cells and entire crypts
- This approach allows us to simulate cancerous field spread in clinically relevant tissue areas consisting of up to 40000 crypts
- Our model simulations suggest a process of mutated cells spreading through the flat mucosa only, without invading neighbouring crypts.
- Our predictions of mutated field size are in accordance with those from published in vivo studies

Keywords

Agent-based modelling, colorectal cancer, multi-scale modelling, simulation

Introduction

Field Cancerisation in the human colon

The human colon consists of a monolayer epithelium punctuated by test-tube shaped invaginations known as the crypts of Lieberkühn. These crypts act as cell factories to supply the large number of cells required to maintain an epithelium in the hostile environment of the colon, necessitating a constant process of division and differentiation within the colon. Disruption of these processes is implicated in the formation of colorectal cancers (CRC) [1].

Changes to the Adenomatous Polyposis Coli (APC) gene, and expression of its associated protein, are strongly linked to the initial stages of adenoma formation [2]. A number of changes to cell behaviour are associated with mutation of this gene including: reduction in cell rigidity, a decrease in the quiescent time before cell cycle re-entry, and increased resistance to anoikis [3].

There is strong evidence that individual crypts are monoclonal in nature; this has been shown through studies on chimeric mice [2] and in an XO/XY mosaic human [4]. The mechanism behind this monoclonal conversion has been elucidated and examined via computational modelling techniques [5, 6]. By contrast, *in vivo* studies [2, 4] have suggested that adenomas are almost exclusively polyclonal in nature, although alternate explanations have been proposed [4]. This, combined with the monoclonality of individual crypts, suggests that multiple crypts are involved in the formation of adenomas. These processes are difficult

to observe in vivo, as they occur over spatial and temporal scales which make them inaccessible to biological techniques, and hence are poorly understood.

A number of studies [7, 8] have suggested that fields of tissue exist around adenomas which are endoscopically normal but exhibit alterations at lower scales and have increased risk of further adenoma formation [9] this falls within the concept of field cancerisation [10]. There are two principal competing hypotheses in the literature as to the mechanism behind field spread. The top-down hypothesis [11] proposes that proliferative advantages caused by the pre-cancerous mutations present in cells from that original crypt invade neighbouring healthy crypts. Once this invasion has occurred the proliferative advantage of the mutated cells allows them to take over the neighbouring crypt by subverting the process of monoclonal conversion, thereon progressively expanding through the local mucosa.

The bottom up hypothesis [12] is centred around the process of crypt fission. This process occurs in healthy tissue as a normal part of epithelial homeostasis. Fission is accelerated by an order of magnitude in tissue of patients with a number of diseases related to CRC [13] so it is hypothesised that crypts with pre-cancerous mutations have an elevated rate of crypt fission. This in turn causes mutated crypts to clone themselves at a higher rate than the homeostatic replacement rate, leading to an expanding patch of mutated tissue. This is currently the most strongly supported of the two hypotheses following both experimental and single crypt-scale computational studies [14, 15].

To date, the direct influence of multiple aspects of cellular phenotype on adenoma formation has not been investigated by computational simulation, possibly due to data scarcity, and also the computational demands of modelling across multiple scales.

Computational Modelling of the Colon Crypt

The colon crypt has been the focus of numerous computational and mathematical modelling studies, with varying scales of resolution. Relatively computationally undemanding

approaches include compartment-based models, which represent sub-populations of stem, transit amplifying and differentiated cells [16] and in the case of the colon, the effects of asymmetric cell division [17] and the enteroendocrine cell population [18]. These concepts were extended to include spatial localisation of these sub-populations in continuum models [19] or applied to model the effects of biomechanical stress [15]. Other approaches based on spatial discretisation include Cellular Automata (CA) models, which have been used in order to study intra-tumour heterogeneity on the scale of the whole colon [20].

Given the importance of cellular phenotype in determining crypt behaviour, more recent work has focussed on the representation of cells as individual entities capable of explicit interactions. The Cellular-Potts method uses the concept of minimisation of an energy function in order to define cell contacts. This approach has been used to study the emergent effects of differential Ephrin-B receptor density along the crypt axis [21], but have the drawback of being computationally expensive, with a potentially non-intuitive reduction of complex cell behaviours to physics driven concepts. Lattice-based crypt models [22] consider the behaviour of individual cells, but confine their movement to occupying fixed grid sites, meaning that explicit consideration of cell-cell and cell microenvironment interaction forces are not possible.

Agent based models (ABMs) capture the dynamic behaviour of complex systems using *software agents*, with each agent being an autonomous entity directly analogous to real world entities (e.g. individual biological cells in a tissue). Each software agent makes decisions based on its internal state and the local environment but is not governed by an overarching control mechanism. By combining many such agents with a suitable environment, complex behaviours arise which reflect the behaviour of the system being modelled. The “cell as agent” approach fits well, as biological cells act as fundamental units or entities which make decisions based on a combination of their internal state and local environment, with complex behaviours emerging via local coordination. However, agents can also be applied at varying levels of hierarchy in order to capture the outcome of emergent

behaviour. In the biological world, agents have also been used to represent molecules within cells [23] and hierarchical agents applied from the level of cells, through tissues and organ to develop a systemic model of inflammation [24]. In another field of application, the context of economics, hierarchical agents have been used to model households, firms and banks of various sizes [25].

In the context of the colon crypt, the first lattice-free cellular-scale ABM used the concept of cell centres as points connected by springs to represent intercellular forces [26] – an approach adopted by many subsequent crypt models, including the models presented here. More recent models have been applied to elucidate the process behind crypt monoclonality [5], the effects of known pre-cancerous mutations on monoclonal conversion [6],cell migration in the crypt [27] and anoikis [28].

Our previous study [29] considered the impact on the crypt mouth of known changes to the behaviour of cells within the crypt arising from pre-cancerous mutations. One of the predictions of this study was that the mutated cells have a competitive advantage at the crypt mouth and possibly on the flat mucosa which allowed them rapidly to dominate this region. As the crypt mouth is the junction between crypts we hypothesise that this behaviour may have bearing on the processes underlying field cancerisation.

The current study has three main aims:

- To examine the consequences of the behaviours seen in the previous study [29], particularly as related to field spread;
- To assess whether the predictions arising from both the previous and the current study are consistent with *in vivo* findings;
- To study the effect of behaviours identified at multi-crypt level when modelled over clinically-observable spatial scales and a timescale of multiple decades

The process of field cancerisation extends beyond the individual crypt, and hence cannot be captured by a cellular-scale single crypt model. In order to achieve these aims, we initially

extended our cellular scale model to represent multiple crypts in order to simulate the characteristics of spread of mutated cells at a fine scale of resolution. We then developed our macro-scale model (where agents represent individual crypts) and calibrated this against the cell scale model, with encoded mechanisms reflecting the behaviours predicted by the latter. Finally, we introduce the process of crypt fission in order to generate initial predictions relating to field spread at the macroscopic scale.

Materials and methods

Cell level model

An Agent-Based model (ABM), where one computational agent represents one biological cell, [28] was used to investigate phenomena related to field spread in a number of simulation experiments. The existing model was extended from a single crypt into a model of a patch of colonic tissue covering multiple crypts, patches of 5x5, 9x9, and 15x15 crypts have been simulated. A 5x5 simulation is visualised in Fig 1A.

Fig 1.

As previously described [29], this lower-scale model incorporates rules representing some of the known effects of Apc loss on the virtual cells. Specifically, reduced cell stiffness and reduced stem cell quiescent time are modelled by modifying the parameters which control those attributes. Resistance to anoikis is modelled by increasing the strength of a cell's attachment to the basement membrane.

For the current study, an area of flat mucosa was added to the model connecting multiple crypts together and rules were created to allow cells to migrate between crypts based on proximity (Box 1). The extent of the spread of mutated cells throughout a simulation was tracked and plotted.

Box 1

```
For each cell
        For each crypt
                If(distanceTo crypt < distanceToCurrentCrypt)
                        make crypt cell's parent crypt
```

A range of model sizes (in terms of total crypt number) with both reflective (agents impacting the boundary are pushed back with a restoring force) and absorbing (agents reaching the boundary are effectively removed from the model) boundary conditions, were tested to determine any variation in model predictions of field spread according to these factors and

hence the least computationally intensive model that could justifiably be used for a sensitivity analysis. This process is described in Supplementary Material 1.

Crypt-Level model

The second model was created specifically for this study and represents individual crypts as agents. This allows areas of millions of crypts to be simulated over multi-year timescales at the cost of granularity of results, a simulation of 40,000 crypts is visualised in Fig 1B. The rules governing the behaviour of crypts are as follows:

Growth - each wildtype crypt has a life cycle [30] which consists of growing or shrinking at a constant rate until a target length is met. When this length is achieved the next target length is drawn from a normal distribution. Typical behaviour of a crypt within a simulation is shown in Fig 1C.

Fission - if a crypt is longer than a global length threshold, then the crypt divides into two crypts. This threshold and the normal distribution from which target lengths are drawn were calibrated to create a fission rate which matches known biological data [1].

Extinction - if a crypt shrinks below a certain length threshold the crypt will become extinct and be removed from the simulation. This rule is phenomenologically motivated, in that whilst such extinctions have not been reported in the literature, it is not obvious how they could be observed. The motivation for the extinction rule is a baseline assumption of global crypt homeostasis: without it, the known rate of crypt fission predicts a full order of magnitude increase in crypt density over a four decade span and no such increase has been observed. These three rules are summarised in Box 2 and Fig 1C.

Box 2

```
For each crypt
    If(Crypt Isn't Mutated)
        If(Length < target)
            Length += growthRate
        Else
            Length -= growthRate
        If(Length > divisionThreshold)
            Divide
        If(Length < 0)
            Remove from Simulation

    Else If(Crypt Is Mutated)
        Length += growthRate
        If(Length > divisionThreshold)
            Divide
```

If a crypt is designated as mutated, its lifecycle will change to one of constant growth and division cycles (Box 2). This calibrated behaviour produces a crypt division rate for mutated crypts which is approximately 20x higher than for wildtype crypts which matches known biological data [1].

Crypts can move over the two-dimensional surface and use a damped spring model to prevent crypts from overlapping. This model is similar to the one used to resolve cell-cell overlaps in the cell scale model and obeys Eq1**:**

$$\mathbf{v} = ((r_1 + r_2 - |\mathbf{p}_1 - \mathbf{p}_2|) * ((\mathbf{p}_1 - \mathbf{p}_2) / |\mathbf{p}_1 - \mathbf{p}_2|) * k) \text{ if } |\mathbf{p}_1 - \mathbf{p}_2| < r_1 + r_2 \quad (1)$$

Where v is the velocity of the crypt for this timestep, $\mathbf{p}_1$ and $\mathbf{p}_2$ are the positions of the two cells and r_1 and r_2 are their radii (Fig 1D).

Crypts can be defined as either wild-type or mutated (i.e. a cell within the crypt has at some point in the past mutated and come to colonise the crypt through monoclonal conversion [5]. When a crypt is designated as mutated, a variable representing the percentage of mutated cells within the flat mucosa above the crypt is incremented each timestep by either a fixed

amount or an amount drawn from a normal distribution to represent mutated cells flowing into the flat mucosa from the mutated crypt below (Box3).

Box 3

```
For each crypt
        If (Crypt Is Mutated)
                Mucosal Mutation Amount += Mutated Cell Production Rate
```

If the flat mucosa contains more than 90% mutated cells, these cells will begin to overflow into the flat mucosa associated with neighbouring crypts. This is implemented via a rule which, for each pair of neighbouring crypts, moves a number of mutated cells from the flat mucosa above the crypt with the higher mutation percentage to the flat mucosa above the crypt with the lower mutation percentage (Box 4).

Box 4

```
For each crypt
        For each NeighbourCrypt
                If (Mucosal Mutation of Either Crypt > 90%)
                        Number of Cells Migrating = Difference in Mucosal
                        Migration * Flow Constant
                        Largest Mucosal Migration -= Number of Cells Migrating
                        Smallest Mucosal Migration += Number of Cells Migrating
```

If a crypt moves beyond the simulation boundary in the y dimension a restoring force is applied proportional to the distance beyond the boundary that the crypt has moved. This creates a fixed boundary in the y dimension to represent the ends of the colon.

If a crypt moves beyond the simulation boundary in the x dimension it is moved to the other side of the simulation plane. This forms a wraparound boundary to simulate the colon as an open ended cylinder (Box 5).

Box 5

```
For each crypt
        If (Crypt.x is Beyond x Boundary)
                Move Crypt to Opposite Side of Simulation
        If (Crypt.y is Beyond y Boundary)
                Apply Restoring Force
```

Crypts along one side of the simulation boundary in the x dimension can interact with crypts on the other side to complete the wraparound conditions. These interactions apply both to crypt overlap resolution forces and to the mucosal mutation spread rules.

The cell scale model was used to conduct a number of simulation experiments relating to the spread of cells exhibiting Apc loss, denoted as *Cell Experiment 1, 2* etc. Following a calibration process, the results of these simulations were then used to inform the upper scale model, which was used to conduct simulations representing a macroscopic section of colon, described below in Crypt Experiment 1.

All cell-level model parameters are shown in Table 2 in [28]. Table 1 below contains the parameters used for the crypt experiments.

Parameter	Value
Simulation width	200 crypts
Simulation height:	20,000 crypts
Simulation time step	8 hours
Crypt growth per time step	0.02 (arbitrary units)
Crypt fission threshold	1 (arbitrary units)
Crypt extinction threshold	0 (arbitrary units)
Mean time to wildtype crypt fission	20 years
Mean time to mutated crypt fission	2 years

Table 1 – Parameters for crypt-as-agent simulations

Results

Modelling Apc loss in a multi-crypt environment predicts invasion of the flat mucosa by precancerous cells

Cell Experiment 1 was a phenomenological investigation of the behaviour of mutated cells within a multi-crypt model. This was initialised as an array of 5x5 crypts and run for 1000 timesteps to reach an equilibrium state. At this point, one cell in the centre crypt of the array was designated as mutated and then the simulation was observed for a further 500000 timesteps. Wildtype cells were coloured red and mutated cells green so that the behaviour of the two populations could be visualised separately. Results are shown in Fig 2A.

Figure 2

The primary prediction of this simulation experiment is that cells carrying a mutation causing APC loss spread through the flat mucosa of neighbouring crypts but do not invade the neighbour crypts themselves. This general prediction held for all of the 625 simulations performed in cell experiment 2 (a mutation rate parameter sensitivity exploration, as described below). A representative visualisation of the simulation is provided in Fig 2A showing mucosal field spread in a typical simulation.

There are relatively few studies yielding candidate biomarkers of Apc loss suitable for immunohistochemical analysis of colorectum, however an *in vitro* study using otherwise isogenic cell lines yielded keratin 18 as one such potential biomarker [31]. Work undertaken previously by this group [32, 33], has also identified keratins as perturbed in macroscopically normal colon in the presence either of a lesion or of pathological inflammation. Immunohistochemical scoring protocols for keratin expression in tissue [34] were therefore applied to assess variability in keratin 18 expression in crypts and flat mucosa of normal tissue in patients with and without lesions (Fig 2B) as a proxy for alteration in Apc. This analysis demonstrated that there was altered expression in the flat mucosa but not the crypt (Fig 2B/C), agreeing with the computational predictions.

Different mutation effects induce field cancerisation at different rates

Following a process to determine the least computationally intensive modelling configuration giving acceptable results (Supplementary Material 1), Cell Experiment 2 examined the effect

of differing parameters associated with the changes related to Apc mutation on the nature of the field spread between crypts. Three parameters pertaining to individual cells designated as mutated cells were varied: the quiescent time of stem cells, the stiffness of the cells, and their resistance to anoikis.

Parameter ranges explored for stem cell quiescent time were 10%, 25%, 50%, 75% and 100% of wild-type value, cell stiffnesses were 10%, 25%, 75% and 100% of wild-type and anoikis resistance was set to 1, 2.5, 5, 7.5, and 10 on an arbitrary scale. All possible combinations of these parameters were tested leading to 125 simulations, each of which was repeated five times to account for stochasticity for a total of 625 simulations, requiring a total of approximately 12,000 hours of compute time on the University of Sheffield multi-core research HPC cluster.

The simulations were run, as in experiment1, for approximately one year of biological time and maximum mutated cell migration distance was recorded. In addition, the originating crypt of a mutated cell population was tracked and any cell achieving a depth of 25% or greater in a crypt from which it did not originate would be considered to have invaded that crypt. These invasion events were logged and recorded along with the migration data to determine if any biologically realistic set of parameters would lead to crypt invasion.

The mean of the spread rate for each simulation was plotted against time and three common predictions were identified. The first is that there is a lag between the mutation event and the onset of field spread; the second is that the fields eventually reach a maximum size and stop spreading, and the third is the rate at which the fields reach this maximum size. These three features were extracted from the data for each combination of parameter values and plotted to determine the contribution of each mutation effect to each feature (Fig 3A). In all cases, each value of the quiescent time modification parameter was plotted as an individual plane of results, with the attachment force parameter plotted on the x-axis, the cell stiffness plotted on the y-axis and the feature being measured plotted on the z-axis.

Figure 3

Fig 3B shows that the quiescent time modification parameter had the largest effect on lag time, with lower quiescent times causing lower lag times. Reducing cell stiffness also affected lag time, with stiffer cells having shorter lags; this effect was emphasised for higher quiescent times. Attachment force did not appear to play a role in lag time.

As shown in Fig 3C**,** quiescent time change has no effect on the overall size of the field generated. Attachment force and cell stiffness both affect total field spread, increasing stiffness reduces the overall size of the field whereas increasing attachment force increases the final field size.

Fig 3D shows the effects of the parameters under test on the rate of field spread. The results can be separated by quiescent time change but the effects appear to be inconsistent. Attachment force and cell stiffness appear to have interrelated effects, with maximal rates of spread occurring at high attachment force when there is low stiffness and low attachment force when there is high stiffness. Parameter sets where both attachment force and cell stiffness are low correspond to minimal spread rate, as do ones where both mutation effects are high.

A key result is that invasion of neighbouring crypts (as opposed to their flat mucosa) was not seen for any physiological combination of values tested. It was, however observed in a small number of combinations tested outside this biologically plausible range, specifically in one repeat of each of the following parameter sets:

Cell stiffness 175%, quiescent time 10%, anoikis resistance 1.0

Cell stiffness 200%, quiescent time 25%, anoikis resistance 2.5

Cell stiffness 200%, quiescent time 25%, anoikis resistance 1.0

Cell stiffness 200%, quiescent time 100%, anoikis resistance 2.5

The biological implications of these values will be considered in the discussion section.

The mean field spread rates obtained from the cell experiments above were then used as parameters in the following crypt level simulations.

Calibrating the Mucosal Invasion Mechanism in the Crypt Scale Model

In order to carry out simulations using the crypt scale model, it was first necessary to determine consistency in the mucosal invasion mechanism in the crypt scale model and also to calibrate the mutated cell production parameter. In order to do this, mechanisms not present in the cell scale model - specifically the crypt fission cycle and movement - were disabled in the higher level model.

An array of six by six crypts was created in both the cell scale model and the crypt scale model. After reaching equilibrium, the crypt at the (2,2) position (using 0-indexing) was designated as *mutated* and the spread of mutation originating from this crypt was tracked. In the crypt scale model, a crypt's flat mucosa was considered to have been colonised when its mutated cells percentage reached 50%. The distance from the mutated (2,2) crypt to each crypt with invaded flat mucosa was calculated and the maximum distance was recorded at every timestep, as a measure of the spread of mutated cells in this model.

Five crypt scale simulations were run with different values for the number of mutated cells produced by the mutated crypt each iteration: 10, 20, 30, 40, and 50 cells per timestep. The simulations were run for approximately one year of biological time. This required only five hundred timesteps for the crypt scale model, as opposed to one million for the cell scale simulations. Fig 4A shows a visualisation of the crypt scale model, consisting of the mutated central crypt with a surrounding region of invaded flat mucosa, which is consistent with the predictions of the cell scale model (Fig 2A). The effect of varying the number of mutated cells generated per timestep in the crypt model is shown in Fig 4B, along with the similar

results from a typical simulation generated using the cell level model (error bars calculated on the basis of five repeat simulations are shown). It can be seen that the mutation spread for the crypt scale model has the same characteristic period of rapid expansion which falls off over time, as is the case for the cell scale model. Additionally, spread rate is predicted to vary based on the value of the cell generation parameter in the crypt scale model and good agreement with the predictions of the cell level model can be achieved by choosing a value of 30 cells per timestep. This parameter was used in subsequent simulations of macroscopic colon tissue described below.

Figure 4

The crypt level model predicts a field of mutated crypts surrounded by a larger field of mutated mucosa

Crypt Experiment 1 was run with the crypt scale model, with crypt fission and movement rules enabled, to examine the spread of mutated cells and crypts over biologically relevant scales. The model was initialised with an array of two hundred crypts in each dimension, giving a total of forty thousand crypts, or approximately 1% of a human colon [1]. The simulation was run for ten thousand timesteps to represent the dynamic state of a colon in an individual of twenty years, at which point a single crypt near the centre of the simulation was mutated. The simulation was then run for a further two decades of biological time and the spread of both mucosal invasion and mutated crypts was measured. These data were recorded every ten timesteps and then plotted against time to characterise the predicted spread. Five repeat simulations were run to account for stochasticity in the crypt cycle.

This experiment predicted a growing field of mutated crypts which displaces the wild-type crypts of the healthy tissue as it grows, as shown in Fig 5A. The expansion of this field accelerates over time in an exponential manner. The experiment also predicted a larger field surrounding the mutated crypts, which consisted of wild-type crypts with mutated flat mucosa. This field initially grows faster than the field of mutated crypts and creates a fringe

around the fully mutated field. The expansion of the flat mucosal field is also exponential, but with a slower growth rate than the field of mutated crypts, the result being that the fringe of invaded flat mucosa becomes thinner as its diameter increases (Fig 5B). The mean size of a field at the end of the simulations was 230 crypts in diameter, which corresponds to approximately 41,000 crypts in total.

Discussion

We have demonstrated how a split scale modelling approach can be used to explore mechanisms of field spread of Apc mutated cells in the colon. The first part of this study investigated the behaviour of APC loss cells in a multi-crypt environment to examine the hypothesis that the competitive advantage conferred by APC loss at the crypt mouth would lead to invasion of neighbouring crypts. Such invasion has been hypothesised in the literature, with arguments being made both for [11] and against [12] this mechanism, however the in-vivo evidence is ambiguous and no modelling studies which address this issue have been previously published.

Our cell scale simulation experiments focussed on predicting emergent behaviour resulting from individual cells exhibiting various phenotypic characteristics of Apc loss, interacting with normal cells in the crypt mouth and specifically, whether transformed cells could migrate outside their crypt of origin, leading to wider tissue invasion. Cell Experiment 1 predicted that there was no top-down invasion of crypts but that mutated cells did invade the flat mucosa above and surrounding neighbouring crypts. This method of field spread does not appear to have been suggested before in the literature and may be a novel process in the understanding of field cancerisation. A study of the literature led us to assess variation in in keratin 18 (a candidate marker for APC loss, [31], in crypts and flat mucosa. Availability of formally recognised biomarkers of Apc loss is a limitation not only of this study, but in the wider literature. Based on our data, the differences in keratin 18 perturbation in patients with an adenoma compared to those without, is consistent with the prediction of APC loss cells in

the flat mucosa surrounding adenomas but not in the crypts at the same location This similarity in the predicted flat mucosal localisation suggests that this mechanism may indeed dominate *in vivo* and follow-up work should be done to determine if this is the case and to what extent these cells could participate in carcinogenic processes.

Cell Experiment 2 sought to quantify the relationship between the three phenotypic effects of APC loss represented in the model and the characteristic properties of field spread. This parameter exploration showed a number of relationships between effects and characteristics which can be explained by the mechanisms at play in the crypt. Lag between initial mutation events and flat mucosal invasion was affected by stem cell quiescent time, with a shorter quiescent time leading to a shorter lag. This relationship is as expected, and due to the fact that a shorter quiescent period gives a competitive advantage in the stem cell niche, reducing the time taken for monoclonal conversion to occur [29], and hence the time until mutated cells emerge from the crypt onto the flat mucosa. Our model also predicts that stiffer cells have lower lag times, due to the fact that stiff cells are driven up the side of the crypt more quickly by the mitotic pressure which drives passive migration in the crypt.

Spatial spread had no discernible relationship with stem cell quiescent time. This can be explained by the fact that quiescent time has very little effect on overall cell production rates as the majority of mitosis occurs in cells which do not undergo a quiescent phase. Increased attachment force led to increasing spatial spread, as high attachment force provides a competitive advantage that allows mutated cells to invade the flat mucosa [29]. Reducing the cell stiffness also caused an increase in spread rate. This is due to the forces which cause anoikis being moderated by the lower stiffness of the mutated cells, which again, gives the mutated cells a competitive advantage in the crypt mouth and flat mucosa.

Rate of spread also did not appear to be affected by quiescent time, again because stem cell quiescent time has negligible effect on cell production rates in the crypt. Low cell stiffness combined with high attachment force gave rise to the largest spread rate, and is driven by

the same mechanisms. There was, however, a secondary maximum in spread rate which corresponded to low attachment force and high cell stiffness. The mechanism which causes this is unknown, but may be related to the phenomenon that, as the number of cells required to achieve a given amount of overall spread is quadratic in the distance of spread so the initial expansion is rapid and falls off with distance.

No parameter combination explored in Cell Experiment 2 led to crypt invasion, suggesting that, in mechanical terms, such events are extremely unlikely with biologically plausible parameters. In particular, the upwards pressure created by the passive migration of cells arising from stem cells' mitoses in neighbouring crypts, and in lieu of chemoattractant signalling mechanisms actively attracting cells to enter these crypts, cells tend to migrate laterally on the flat mucosa. An implication of this model is that the "top down" hypothesis of field spread [11] may not be the primary mechanism prevalent during colon cancerisation.

It was, however, discovered through a wider parameter exploration that greater than normal cell stiffness occasionally gave rise to crypt invasion. This is unlikely to happen mechanically as cancerous cells are generally understood to be less stiff than wildtype [3]. This is a function of the switch from keratin to vimentin as primary component of intermediate filaments [35, 36]; our group have shown alterations in keratin-vimentin ratio in the colorectal mucosa in cancer-predisposing colitis [37] and around pre-malignant colorectal lesions [33]. However, it is possible that a signalling mechanism could potentially create a similar effect. It is known that EphB signalling mediates cell-cell adhesion forces in order to create a sorting mechanism within the crypt [38], and a disruption of this mechanism could potentially create an advantage for mutated cells very similar to that seen by increasing cell stiffness beyond normal levels. This would be an attractive target for future modelling efforts, as it is relatively straightforward to incorporate such a signalling mechanism into the current model. In addition, should evidence for a signalling mechanism actively attracting mutated cells to actively invade wildtype crypts arise, it is possible that inclusion in our model could give rise to predictions of top-down invasion. Research in this

area remains relatively novel and piecemeal in the cancer area [39], but as evidence consolidates, this feature will be included in our model.

Crypt Experiment 1 predicted a two-phase field growing from a single mutated crypt. The first phase was a fringe of invaded flat mucosa, which initially expanded more quickly than the second phase, a core of fully mutated crypts. The invaded mucosa eventually created a fringe ten crypts wide, before contracting to a narrow zone around the fully mutated region. This later contraction is most likely a geometrical effect, as the field expands the area required to grow the mucosal field grows as the square of the radius of the field but the number of mutated cells being created to invade that area only grows linearly with the radius of the fully mutated field. This acts as a brake on the expansion of the mucosal field.

This experiment appears to be the first time that a growing field has been modelled at this scale and over an extended period of time. The total number of mutated crypts was approximately 41,000 which is in good agreement with the sizes of fields reported in-vivo in the literature [1]. At the end of our simulation of field expansion, the field remained in exponential growth after the equivalent of two decades of biological time, achieving a virtual diameter of around 40mm, which is a scale that would fall within the clinically observable range. This field size is broadly in agreement with previous estimates [1], however if unchecked the field would presumably continue to expand. There are a number of limitations of this model: the reference data for achieved field size are from ulcerative colitis rather than sporadic adenoma; the parameterisation of crypt fission rate is a best estimate from a single study of an elusive biological process, and the data acquired in mice. Future *in silico* studies might undertake parameter explorations at the upper scale to establish the effect of small changes in crypt fission rates on field growth, and the relative contributions of fission and Apc- cell invasion to overall field size. For instance, the values for crypt fission or death that give rise to clonal patches consistent with studies of X-inactivation [40] could be explored. Further studies *in vivo* may yield improved parameters for these processes allowing model refinement. Notwithstanding these limitations, the timelines from risk exposure to modest

size field seem in accord with some epidemiological data [41] which suggest the exposure-presentation window is in the decades timeframe.

There is potential for further work to be done both *in-vivo* and *in-silico* to refine and validate the model to produce more detailed and accurate field spread predictions, which could potentially have clinical or prognostic uses. As the model can simulate clinically-relevant spatial scales, over a two-decade time span in only 12 hours of computational time, there is great scope for doing extensive studies such as simulating populations and cohorts to examine statistical outcomes of changes between groups, for example under different treatment regimes or long-term lifestyle nutrition interventions which would be prohibitively time-consuming to study *in-vivo*. Extending our 40000 crypt model to represent a truly organ scale is underway; this 4 million crypt model is being assessed for potential to explore the basis of polyclonal adenoma formation.

Further possibilities include the use of the model to explore the concept of interactions of clones arising from subsequent mutations within an advancing field or entirely independent primary mutations arising from different crypts. Previous simulations carried out by Sottoriva et al using a cellular automata-based model capturing the probabilities of the fission or extinction of individual glands according to their mutation status have produced results suggesting that the earliest mutations are dominant within adenomas,and shown to be in agreement with experimental data [20]. Our approach, capturing phenotypic behaviours on the cellular scale, will allow exploration of the role of a diverse range of intra- and inter-crypt behaviour on field expansion and clonal interaction.

Conclusions

This study has used two agent based models and *in vivo* data to investigate the spread of pre-cancerous fields in the colonic epithelium. The key findings are:

- The cell level model predicts that mutated cells will spread through the flat mucosa above wildtype crypts, but that invasion of neighbouring crypts will not occur. *In vivo* biopsy data suggests that this is indeed the case.
- The crypt level model produces predictions in line with those of the cell level model, but is efficient enough to be run at clinically-relevant scales for multiple decades of biological time.

Our work has generated predictions leading to further questions regarding the nature of field spread in the human colon, some of which may be targets for future *in vivo* or *in vitro* (e.g. using organoids). However, the ability to run computational simulations of the colon on time and length scales associated with *in vivo* cancer development opens up future possibilities for clinically relevant *in silico* exploration.

References

1. Humphries, A. and N.A. Wright, *Colonic crypt organization and tumorigenesis.* Nature Reviews Cancer, 2008. **8**(6): p. 415-424.
2. Merritt, A.J., K.A. Gould, and W.F. Dove, *Polyclonal structure of intestinal adenomas in Apc-(Min)/+ mice with concomitant loss of Apc(+) from all tumor lineages.* Proceedings of the National Academy of Sciences of the United States of America, 1997. **94**(25): p. 13927-13931.
3. Sansom, O.J., et al., *Loss of Apc in vivo immediately perturbs Wnt signaling, differentiation, and migration.* Genes & Development, 2004. **18**(12): p. 1385-1390.
4. Novelli, M.R., et al., *Polyclonal origin of colonic adenomas in an XO/XY patient with FAP.* Science, 1996. **272**(5265): p. 1187-1190.
5. Fletcher, A.G., C.J.W. Breward, and S.J. Chapman, *Mathematical modeling of monoclonal conversion in the colonic crypt.* Journal of Theoretical Biology, 2012. **300**: p. 118-133.
6. Mirams, G.R., et al., *A theoretical investigation of the effect of proliferation and adhesion on monoclonal conversion in the colonic crypt.* Journal of Theoretical Biology, 2012. **312**: p. 143-156.
7. Bernstein, C., et al., *Field defects in progression to adenocarcinoma of the colon and esophagus.* EJB Electronic Journal of Biotechnology, 2000. **3**(3 CITED APRIL27, 2001): p. 1-22.
8. Yu, D.C.W., et al., *Short-chain fatty acid level and field cancerization show opposing associations with enteroendocrine cell number and neuropilin expression in patients with colorectal adenoma.* Molecular Cancer, 2011. **10**.
9. Patel, A., et al., *Field cancerisation in colorectal cancer: A new frontier or pastures past?* World Journal of Gastroenterology, 2015. **21**(13): p. 3763-3772.
10. Slaughter, D.P., H.W. Southwick, and W. Smejkal, *Field cancerization in oral stratified squamous epithelium; clinical implications of multicentric origin.* Cancer, 1953. **6**(5): p. 963-8.
11. Shih, I.-M., et al., *Top-down morphogenesis of colorectal tumors.* Proceedings of the National Academy of Sciences of the United States of America, 2001. **98**(5): p. 2640-2645.
12. Preston, S.L., et al., *Bottom-up histogenesis of colorectal adenomas: Origin in the monocryptal adenoma and initial expansion by crypt fission.* Cancer Research, 2003. **63**(13): p. 3819-3825.
13. Cheng, H., et al., *CRYPT PRODUCTION IN NORMAL AND DISEASED HUMAN COLONIC EPITHELIUM.* Anatomical Record, 1986. **216**(1): p. 44-48.
14. Kershaw, S.K., et al., *Colorectal cancer through simulation and experiment.* IET Systems Biology, 2013. **7**(3): p. 57-73.
15. Edwards, C.M. and S.J. Chapman, *Biomechanical modelling of colorectal crypt budding and fission.* Bulletin of Mathematical Biology, 2007. **69**(6): p. 1927-1942.
16. Tomlinson, I.P.M. and W.F. Bodmer, *Failure of Programmed Cell-Death and Differentiation as Causes of Tumors - Some Simple Mathematical-Models.* Proceedings of the National Academy of Sciences of the United States of America, 1995. **92**(24): p. 11130-11134.
17. Johnston, M.D., et al., *Mathematical modeling of cell population dynamics in the colonic crypt and in colorectal cancer.* Proceedings of the National Academy of Sciences of the United States of America, 2007. **104**(10): p. 4008-4013.
18. Smallbone, K. and B.M. Corfe, *A mathematical model of the colon crypt capturing compositional dynamic interactions between cell types.* International Journal of Experimental Pathology, 2014. **95**(1): p. 1-7.
19. Murray, P.J., et al., *Modelling Spatially Regulated beta-Catenin Dynamics and Invasion in Intestinal Crypts.* Biophysical Journal, 2010. **99**(3): p. 716-725.
20. Sottoriva, A., et al., *A Big Bang model of human colorectal tumor growth.* Cancer Research, 2015. **75**(22).

21. Wong, S.Y., et al., *Computational model of cell positioning: directed and collective migration in the intestinal crypt epithelium.* Journal of the Royal Society Interface, 2010. **7**: p. S351-S363.
22. Bravo, R. and D.E. Axelrod, *A calibrated agent-based computer model of stochastic cell dynamics in normal human colon crypts useful for in silico experiments.* Theoretical Biology and Medical Modelling, 2013. **10**: p. 24.
23. Pogson, M., et al., *Introducing Spatial Information into Predictive NF-kappa B Modelling - An Agent-Based Approach.* Plos One, 2008. **3**(6).
24. An, G., *Introduction of an agent-based multi-scale modular architecture for dynamic knowledge representation of acute inflammation.* Theoretical Biology and Medical Modelling, 2008. **5**.
25. Deissenberg, C., S. van der Hoog, and H. Dawid, *EURACE: A massively parallel agent-based model of the European economy.* Applied Mathematics and Computation, 2008. **204**(2): p. 541-552.
26. Meineke, F.A., C.S. Potten, and M. Loeffler, *Cell migration and organization in the intestinal crypt using a lattice-free model.* Cell Proliferation, 2001. **34**(4): p. 253-266.
27. Dunn, S.-J., I.S. Naethke, and J.M. Osborne, *Computational Models Reveal a Passive Mechanism for Cell Migration in the Crypt.* Plos One, 2013. **8**(11).
28. Ingham-Dempster, T., D.C. Walker, and B.M. Corfe, *An agent-based model of anoikis in the colon crypt displays novel emergent behaviour consistent with biological observations*. 2017, The Royal Society Publishing: Royal Society Open Science.
29. Ingham-Dempster, T., B. Corfe, and D. Walker, *A cellular based model of the colon crypt suggests novel effects for Apc phenotype in colorectal carcinogenesis.* Journal of Computational Science, 2018. **24**: p. 125-131.
30. Wasan, H.S., et al., *APC in the regulation of intestinal crypt fission.* Journal of Pathology, 1998. **185**(3): p. 246-255.
31. Hammoudi, A., et al., *Proteomic profiling of a mouse model of acute intestinal Apc deletion leads to identification of potential novel biomarkers of human colorectal cancer (CRC).* Biochem Biophys Res Commun, 2013. **440**(3): p. 364-70.
32. Corfe, B.M., et al., *A study protocol to investigate the relationship between dietary fibre intake and fermentation, colon cell turnover, global protein acetylation and early carcinogenesis: the FACT study.* Bmc Cancer, 2009. **9**.
33. Evans, C.A., et al., *Reduced keratin expression in colorectal neoplasia and associated fields is reversible by diet and resection.* BMJ Open Gastroenterol, 2015. **2**(1): p. e000022.
34. Khan, A.Q., et al., *Keratin 8 expression in colon cancer associates with low faecal butyrate levels.* Bmc Gastroenterology, 2011. **11**.
35. Terriac, E., et al., *Vimentin Levels and Serine 71 Phosphorylation in the Control of Cell-Matrix Adhesions, Migration Speed, and Shape of Transformed Human Fibroblasts.* Cells, 2017. **6**(1).
36. Rathje, L.S.Z., et al., *Oncogenes induce a vimentin filament collapse mediated by HDAC6 that is linked to cell stiffness.* Proceedings of the National Academy of Sciences of the United States of America, 2014. **111**(4): p. 1515-1520.
37. Corfe, B.M., et al., *Inflammation decreases keratin level in ulcerative colitis; inadequate restoration associates with increased risk of colitis-associated cancer.* BMJ Open Gastroenterol, 2015. **2**(1): p. e000024.
38. Holmberg, J., et al., *EphB receptors coordinate migrationand proliferation in the intestinal stem cell niche.* Cell, 2006. **125**(6): p. 1151-1163.
39. Trevino, E.N.G., et al., *Effects of pericytes and colon cancer stem cells in the tumor microenvironment.* Cancer Cell International, 2019. **19**.
40. Novelli, M., et al., *X-inactivation patch size in human female tissue confounds the assessment of tumor clonality.* Proceedings of the National Academy of Sciences of the United States of America, 2003. **100**(6): p. 3311-3314.

41. Kantor, E.D., et al., *Adolescent body mass index and erythrocyte sedimentation rate in relation to colorectal cancer risk.* Gut, 2016. **65**(8): p. 1289-1295.

Figures

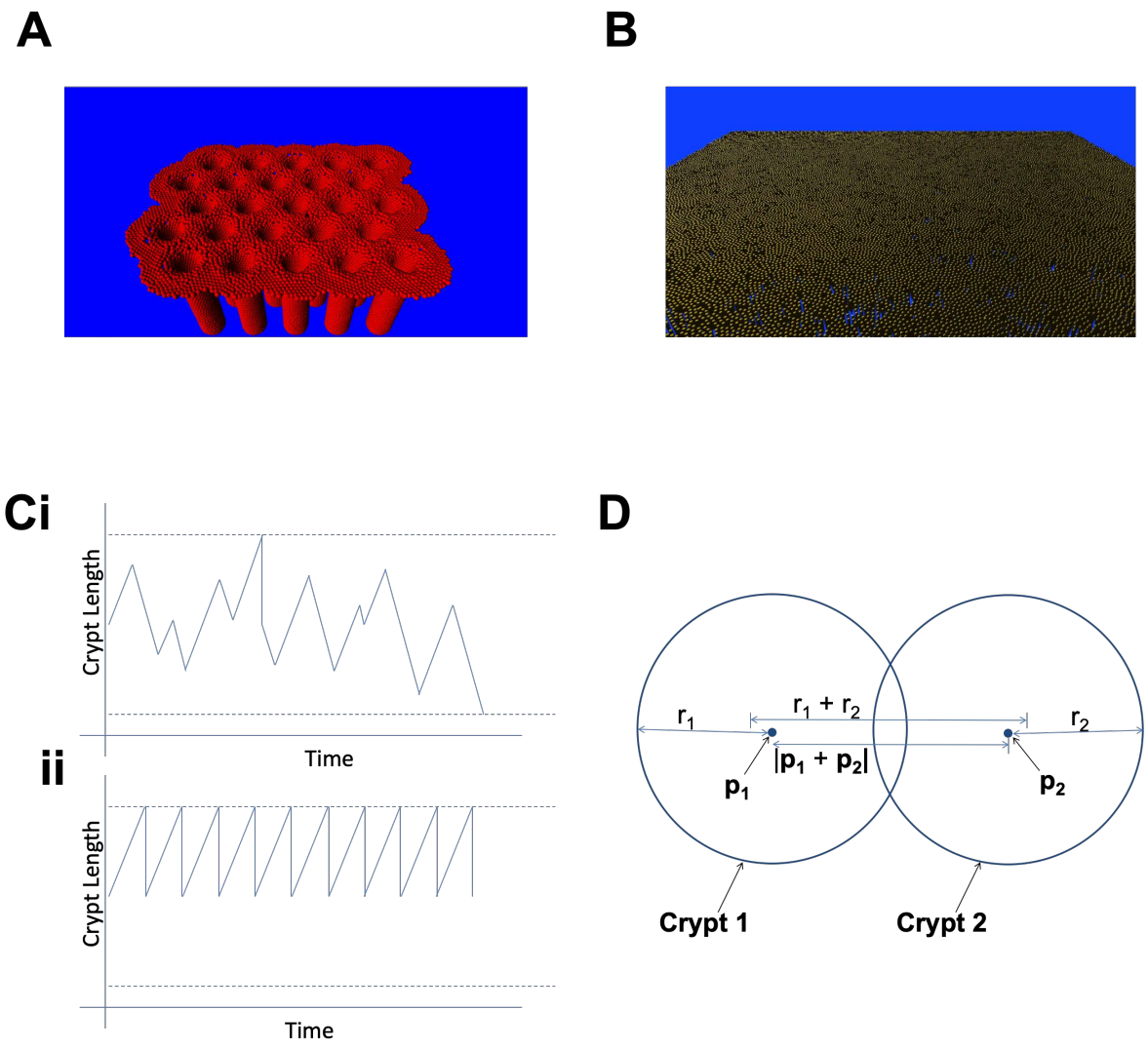

Figure 1 Multicrypt Model Development A: Visualisation of the cell scale model showing an array of 5x5 crypts. **B:** Visualisation of the crypt scale model output showing approximately 40,000 crypts. **Ci:** The crypt cycle of wild-type crypts in the crypt scale model. In this example the crypt would fission once and die at the end of the example timespan, **ii:** The crypt cycle of a mutated crypt, in this example the crypt would fission ten times and never die. **D:** Overlap resolution in the crypt scale model showing the various parameters referenced in Eq1

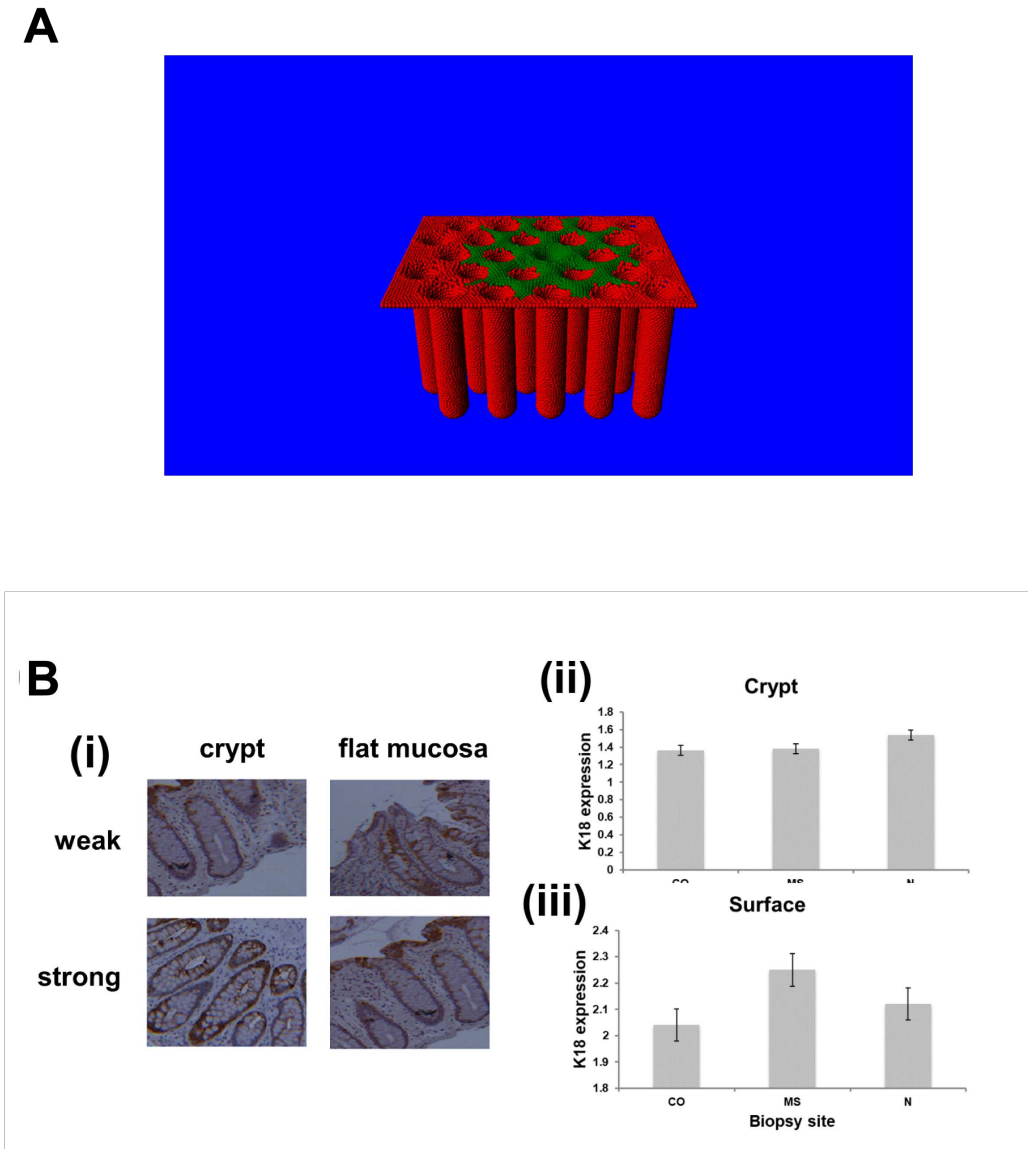

Figure 2 Invasion of the Flat Mucosa. **A:** Visualisation of the cell scale model showing mutated cells (green) from the central crypt invading the flat mucosa above neighbouring crypts (red), note that no mutated cells are present within the neighbour crypts themselves. **B** Alterations in keratin 18 (a biomarker of Apc loss) in the crypt and flat mucosa. (i) immunohistological staining for keratin 18 in crypt and flat mucosa showing examples of weak and strong staining at each location; (ii) comparison of keratin 18 staining in the crypts from patients without lesion adenoma (N) or patients with a lesion (CO and MS samples from same patients, CO from adjacent to lesion, MS from distant to the lesion); (iii) the same samples' scores at flat mucosa

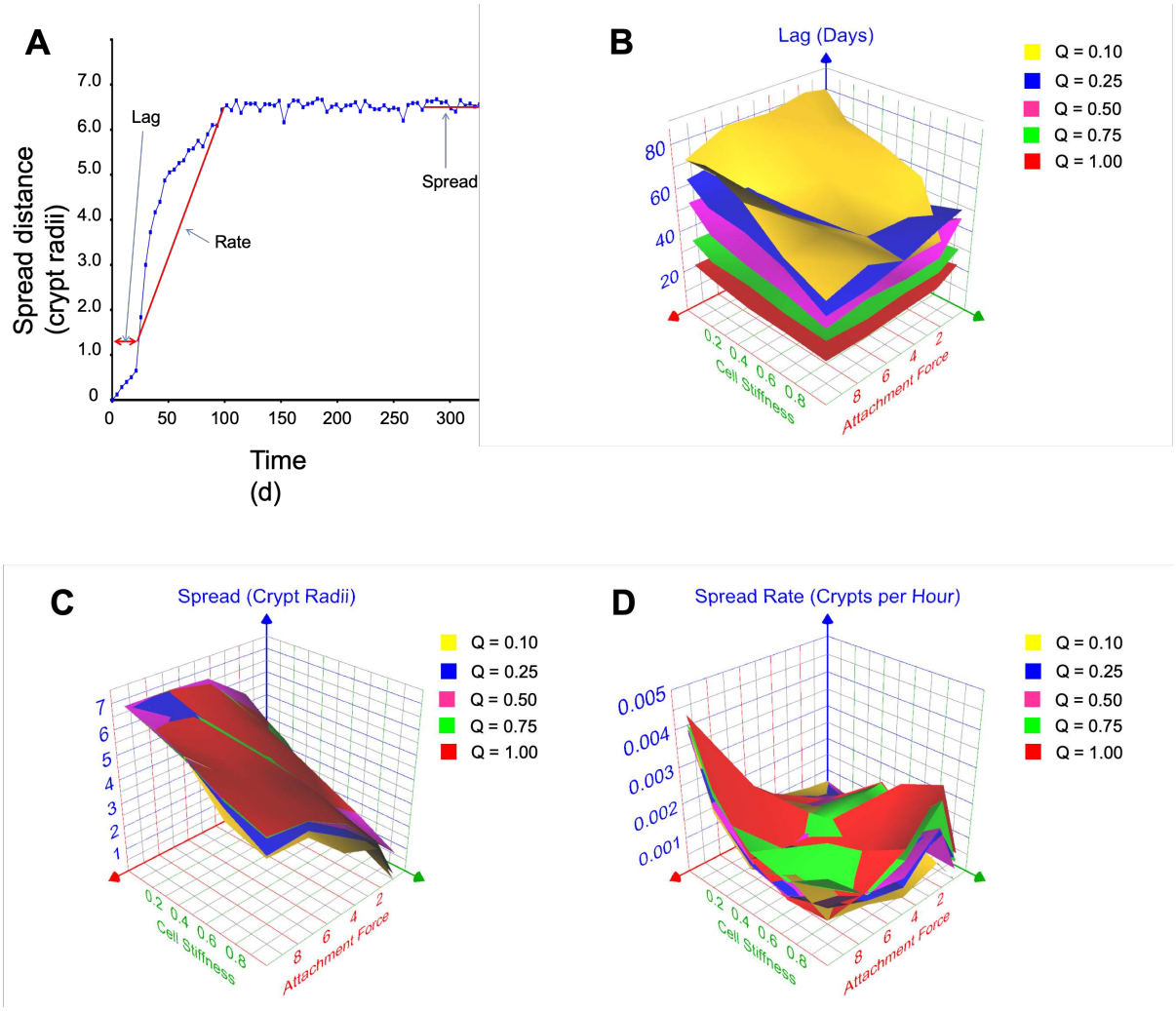

Figure 3 Mucosal Invasion Sensitivity Analysis. **A**: A plot of spread distance against time for a typical simulation showing the three characteristic features measured in the parameter sweep experiment, specifically lag, spread rate, and overall spread distance. **B**: Three dimensional plot showing the effect of quiescent time reduction, attachment force increase and cell stiffness reduction on the lag time before field spread onset. **C**: Three dimensional plot of overall spread resistance plotted by the three mutation effects. **D**: Plots of the effect of quiescent time reduction, attachment force increase, and cell stiffness on the rate of field spread, are shown in Figs 3B, C and D respectively.

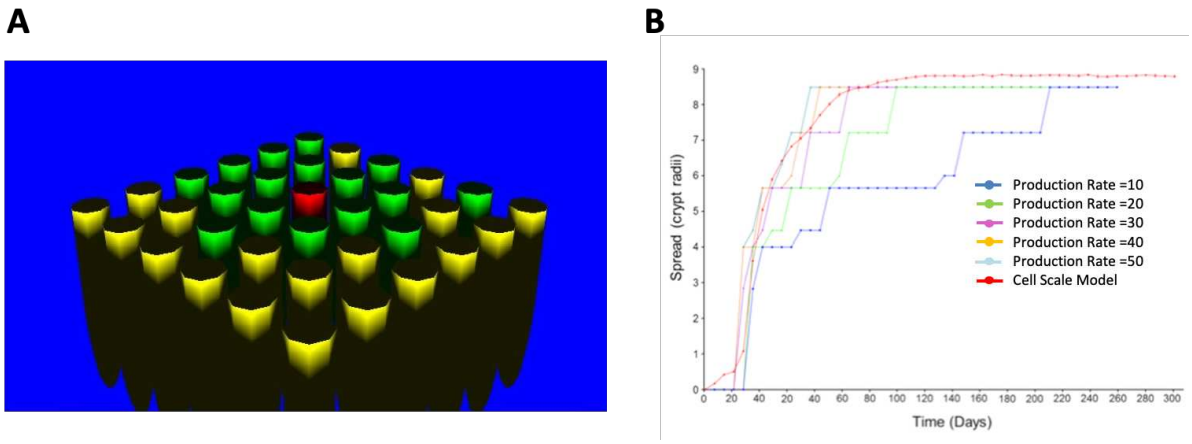

Figure 4 A A visualisation of the crypt scale model after modification for validation against the cell scale model. Yellow crypts are wild-type, red are mutated, and green are wild-type with mutated flat mucosa. **B** Plot of spread against time for the 6x6 cell scale model and the crypt scale model at 6x6 with different choices of mutated cell production parameter

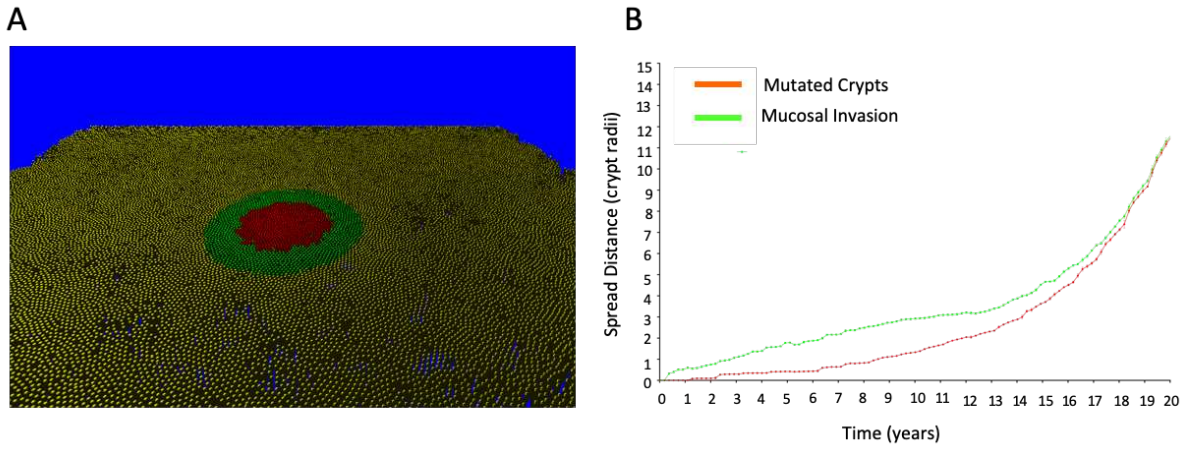

Figure 5 Crypt Scale Simulation Results. **A:** Visualisation of the full sized crypt scale model after a single mutation event showing the growing fields of mutated crypts (red) and invaded mucosa (green). **B**: A plot of spread distance against time for the experiment visualised in A, showing that both fields grow exponentially, with the mucosal field (green) initially growing faster than the fully mutated field (red) which later catches up.

Author Bios

Dr Tim Ingham Dempster has a background in scientific software development and recently completed his PhD at the University of Sheffield in Computational Modelling of Colorectal Cancer. He is now working in the pharmaceutical industry developing drug absorption simulations.

Ms Ria Rosser is a surgical registrar who completed her MD at the University of Sheffield investigating the role of keratin and other proteins in modifying risk of colorectal adenoma recurrence. RR contributed the scoring and analysis of alterations in keratin expression at multiple sites in the mucosa.

Dr Bernard Corfe leads the Molecular Gastroenterology Research Group at The University of Sheffield. His interests are in the role of diet in colorectal diseases including IBS, IBD and cancer, particularly at the molecular scale. BMC co-conceived and co-directed the project with DW.

Dr Dawn Walker is an academic at the University of Sheffield with expertise in the development of agent-based models of biological cells and tissues, including epithelial homeostasis and wound healing, restenosis in vascular systems, fertilisation and colon cancer, as well as integration of ABMs into multiscale tissue models.